

Fluid-fluid phase behaviour in the explicit solvent ionic model: hard spherocylinder solvent molecules

M. Hvozď, T. Patsahan, O. Patsahan, M. Holovko

*Institute for Condensed Matter Physics of the National Academy of Sciences of Ukraine,
1 Svientsitskii St., 79011 Lviv, Ukraine*

Abstract

We study a fluid-fluid phase transition of the explicit solvent model represented as a mixture of the restricted primitive model (RPM) of ionic fluid and neutral hard spherocylinders (HSC). To this end, we combine two theoretical approaches, i.e., the scale particle theory (SPT) and the associative mean spherical approximation (AMSA). Whereas the SPT is sufficient to provide a rather good description of a reference system taking into account hard-core interactions, the AMSA is known to be efficient in treating the Coulomb interactions between the ions. Alternatively, we also use the mean spherical approximation (MSA) for comparison. In general, both approximations lead to similar qualitative results for the phase diagrams: the region of coexisting envelope becomes broader and shifts towards larger densities and higher temperatures when the pressure increases. However, the AMSA and the MSA produce different concentration dependences, i.e., contrary to the MSA, the AMSA phase diagrams show that the high-density phase mostly consists of the ions for all pressures considered. To demonstrate the effect of asphericity of solvent molecules on the fluid-fluid phase transition, we consider an “equivalent” mixture in which the HSC particles are replaced by hard spheres (HS) of the same volume. It is observed that in the case of HSC solvent (RPM-HSC model), the region of phase coexistence is wider than for the case of the solvent molecules being of spherical shape (RPM-HS model). It is also found that the critical temperature is higher in the RPM-HSC model than in the RPM-HS model, though it becomes the same at higher pressures in the MSA, while in the AMSA this difference remains essential.

Keywords: ionic solutions, fluid-fluid equilibrium, explicit solvent model,

1. Introduction

The description of the thermodynamic behaviour of ionic solutions including their phase separation is important in many fields such as biology, electrochemistry, and material science. The simplest model capable of capturing the main features of the systems with electrostatic interactions is the restricted primitive model (RPM). In this model, the ionic fluid is modelled as an electroneutral binary mixture of charged hard spheres (HS) of equal diameter and valency immersed in a structureless dielectric continuum. A major drawback of this model is the use of the solvent continuum assumption in which the effects of solvent structure are totally neglected. The simplest possible model which treats the solvent explicitly is a mixture of the RPM fluid and neutral hard spheres (the RPM-HS mixture). In such a model, the polar nature of the solvent is represented implicitly by a continuum background with a dielectric constant. The RPM-HS mixture undergoes a demixing phase transition in the phases of different ion concentrations. The phase behaviour of the RPM-HS mixture was theoretically studied by using the mean-spherical approximation (MSA) [1] and the pairing MSA (PMSA) [2]. More recently [3], a comparative study of the fluid-fluid phase separation in the RPM-HS mixture has been performed using three theoretical approaches: the random phase approximation (RPA) with the Weeks-Chandler-Anderson regularization of the Coulomb potential (the WCA approximation) [4, 5], the mean spherical approximation (MSA) [6, 7, 8, 9], and the associative mean spherical approximation (AMSA) [10, 11]. The results have demonstrated that the AMSA leads to the best agreement with the available simulation data [12] when the association constant proposed by Olaussen and Stell is used [13].

In this paper, we study the fluid-fluid phase diagram of an ionic solution model in which the solvent molecules are of non-spherical shape. More precisely, we focus on the mixture of the RPM and uncharged hard spherocylinders (HSC) and refer to this system as the RPM-HSC mixture. In order to clarify the effect of asphericity of solvent molecules on the fluid-fluid phase transitions, we also consider a mixture of RPM fluid and "equivalent" hard spheres, which are taken of the same volumes as HSC particles in the

previous case, and refer to this system as the RPM-HS mixture. Therefore, we investigate two similar models, but in the first model (RPM-HSC) neutral solvent molecules are of elongated shape like spherocylinders and in the second model (RPM-HS) neutral solvent molecules are spherical.

For both the RPM-HSC and RPM-HS models, we use the AMSA theory to evaluate the contribution to thermodynamic properties due to electrostatic interactions of the ionic component. According to this theory the ions are considered as a system of free ions and ion pairs which are in a chemical equilibrium defined by the mass action law (MAL) [10, 11, 14, 15]. The AMSA theory reduces to the MSA when the association phenomena between ions is neglected, i.e., ion pairing is not taken into account in the case of MSA. In our study we provide a comparison of the phase diagrams obtained from both the AMSA and MSA theories.

To evaluate the contribution of hard-core interactions to the thermodynamics of the RPM-HSC model, a reliable description of the binary system consisting of neutral HS and HSC particles (HS-HSC mixture) is necessary. For this purpose we apply the scale particle theory (SPT) originally developed by Reiss and coworkers [16, 17] and then extended to anisotropic particles in [18, 19, 20, 21]. Recently [22, 23], the SPT has been developed to the case of a HS-HSC mixture. In [23], analytical expressions for the free energy, pressure and chemical potentials are derived and, on this ground, an isotropic-nematic phase transition in the HS-HSC mixture is studied. Furthermore, the SPT theory was extended to the description of thermodynamic properties and orientation ordering of the HS-HSC mixture confined in a disordered porous medium [24], where the Carnahan-Starling-like correction (CS) and Parsons-Lee (PL) corrections [25, 26] were introduced. With this correction, the analytical expressions for the thermodynamics quantities obtained in the SPT can be turned to the CS formula [27] if the length of HSC particles is set to zero and diameters of HSC and HS particle are equal. This essentially improves the SPT description of the HS-HSC mixture at high densities. In the present paper, we propose a modification of the CS correction, due to which the SPT expressions can be reduced to the Mansoori-Carnahan-Starling-Leland formula [28] if the length of HSC particles is set to zero, while the diameter HSC and HS particles can differ. The PL correction corrects the description of isotropic-nematic transition for spherocylinders of small length. This new formulation of the SPT description for a HS-HSC mixture is used for the reference system in the AMSA and MSA calculations.

The paper is arranged as follows. Section 2 presents the basic model and

theoretical formalism. In Section 3, the results for the phase diagrams are presented and discussed. We conclude in Section 4.

2. Theory

2.1. Model

We consider a model ionic fluid immersed in a solvent consisting of uncharged (neutral) hard spherocylinders (HSC). The HSC consists of a cylinder of length L and diameter D capped by two hemispheres of the same diameter. The ionic fluid is treated as a restricted primitive model (RPM) that consists of an equal number of equisized positively and negatively charged hard spheres. The interaction potentials between two ions are as follows:

$$u_{\alpha\beta}(r) = \begin{cases} \infty, & r < \sigma_1 \\ \frac{Z_\alpha Z_\beta e^2}{\varepsilon r}, & r \geq \sigma_1 \end{cases}, \quad (1)$$

where $Z_+ = -Z_- = 1$, $\sigma_1 = 2R_1$ is the diameter of ions, R_1 is the radius of ions, e is the elementary charge, and ε is the dielectric constant of the solvent. We denote as $\rho_1 = \rho_+ + \rho_-$ the total number density of ions.

In the case when there is no interaction between ions and spherocylinders beyond the hard core, one can present the Helmholtz free energy of the RPM-HSC mixture in the form:

$$\beta F = \beta F^{\text{ref}} + \beta \Delta F^{\text{ion}}, \quad (2)$$

where F^{ref} is the free energy of a reference system, represented by a mixture of hard-spheres and spherocylinders. ΔF^{ion} is the part connected with the ionic subsystem, and $\beta = 1/k_B T$.

2.2. Reference system

We start with the description of the reference system consisting of a binary mixture of hard convex bodies (HCB) of different shape. The HCB can be characterized by a set of three geometrical parameters: the volume V of a particle, its surface area S and the mean curvature r taken with a factor $1/4\pi$ [31]. For the HS particles with the radius R_1 , these parameters are

$$V_1 = \frac{4}{3}\pi R_1^3, \quad S_1 = 4\pi R_1^2, \quad r_1 = R_1. \quad (3)$$

For the HSC particles with the radius R_2 and the length L_2 , we have

$$V_2 = \pi R_2^2 L_2 + \frac{4}{3} \pi R_2^3, \quad S_2 = 2\pi R_2 L_2 + 4\pi R_2^2, \quad r_2 = \frac{1}{4} L_2 + R_2. \quad (4)$$

Using the SPT theory, we can present the equation of state of the HS-HSC mixture in the form:

$$\frac{\beta P^{\text{ref}}}{\rho} = \frac{\beta P^{\text{CS}}}{\rho} = \frac{\beta P^{\text{SPT}}}{\rho} + \frac{\beta \Delta P^{\text{CS}}}{\rho}, \quad (5)$$

where the first addend follows from the SPT [18, 29]

$$\frac{\beta P^{\text{SPT}}}{\rho} = 1 + \frac{\eta}{1-\eta} + \frac{A}{2} \frac{\eta}{(1-\eta)^2} + \frac{2B}{3} \frac{\eta^2}{(1-\eta)^3}. \quad (6)$$

The second addend is the Carnahan-Starling (CS) correction which is introduced to improve the description of the thermodynamics of the HS-HSC mixture at high densities. The correction is chosen in the form [30]:

$$\frac{\beta \Delta P^{\text{CS}}}{\rho} = -\frac{\eta^3}{(1-\eta)^3} \Delta_1. \quad (7)$$

In (6), the following notations are introduced [23]:

$$A = \sum_{\alpha=1}^2 x_{\alpha} a_{\alpha}, \quad B = \sum_{\alpha=1}^2 x_{\alpha} b_{\alpha}, \quad (8)$$

$$a_1 = 6 \frac{\eta_1}{\eta} + \left[\frac{1}{k_1} \frac{6\gamma_2}{3\gamma_2 - 1} + \frac{1}{k_1^2} \frac{3(\gamma_2 + 1)}{3\gamma_2 - 1} \right] \frac{\eta_2}{\eta}, \quad (9)$$

$$b_1 = \frac{1}{2} \left(3 \frac{\eta_1}{\eta} + \frac{1}{k_1} \frac{6\gamma_2}{3\gamma_2 - 1} \frac{\eta_2}{\eta} \right)^2, \quad (10)$$

$$\begin{aligned} a_2(\tau(f)) &= \left[\frac{3}{4} s_1 (1 + 2k_1) + 3k_1 (1 + k_1) \right] \frac{\eta_1}{\eta} + \left[6 \right. \\ &\quad \left. + \frac{6(\gamma_2 - 1)^2 \tau(f)}{3\gamma_2 - 1} \right] \frac{\eta_2}{\eta}, \end{aligned} \quad (11)$$

$$\begin{aligned}
b_2(\tau(f)) &= \left(\left[\frac{3}{4}s_1 + \frac{3}{2}k_1 \right] \frac{\eta_1}{\eta} + \left[\frac{3(2\gamma_2 - 1)}{3\gamma_2 - 1} + \frac{3(\gamma_2 - 1)^2 \delta \tau(f)}{3\gamma_2 - 1} \right] \right. \\
&\times \left. \frac{\eta_2}{\eta} \right) \left(3k_1 \frac{\eta_1}{\eta} + \frac{6\gamma_2}{3\gamma_1 - 1} \frac{\eta_2}{\eta} \right), \tag{12}
\end{aligned}$$

where

$$k_1 = \frac{R_2}{R_1}, \quad s_1 = \frac{L_2}{R_1}, \quad \gamma_2 = 1 + \frac{L_2}{2R_2}, \tag{13}$$

$$\eta = \eta_1 + \eta_2, \quad \eta_1 = \rho_1 V_1, \quad \eta_2 = \rho_2 V_2, \tag{14}$$

$$\rho = \rho_1 + \rho_2, \quad x_1 = \frac{\rho_1}{\rho}, \quad x_2 = \frac{\rho_2}{\rho}, \tag{15}$$

and $\delta = 3/8$ is the PL correction. In Eq.(11)-(12), $\tau(f)$ is given by

$$\tau(f) = \frac{4}{\pi} \int f(\Omega_1) f(\Omega_2) \sin[\gamma(\Omega_1, \Omega_2)] d\Omega_1 d\Omega_2, \tag{16}$$

where $\Omega = (\vartheta, \varphi)$ denotes the orientation of HSC particles and it is defined by the angles ϑ and φ , $d\Omega = \frac{1}{4\pi} \sin \vartheta d\vartheta d\varphi$ is the normalized angle element, $\gamma(\Omega_1, \Omega_2)$ is an angle between orientation vectors of two molecules, $f(\Omega)$ is the singlet orientation distribution function normalized in such a way that

$$\int f(\Omega) d\Omega = 1. \tag{17}$$

The singlet orientational distribution function $f(\Omega)$ can be obtained from a minimization of the free energy with respect to variations of this distribution. This procedure leads to the nonlinear integral equation

$$\ln f(\Omega_1) + \lambda + C \int f(\Omega') \sin(\Omega_1 \Omega') d\Omega' = 0, \tag{18}$$

where

$$C = \frac{\eta_2}{1 - \eta} \left[\frac{3(\gamma_2 - 1)^2}{3\gamma_2 - 1} + \frac{1}{1 - \eta} \frac{(\gamma_2 - 1)^2}{3\gamma_2 - 1} \delta \left(3k_1 \eta_1 + \frac{6\gamma_2}{3\gamma_2 - 1} \eta_2 \right) \right] \tag{19}$$

and the constant λ is defined from the normalization condition Eq.(17).

In (7), Δ_1 is of the form:

$$\Delta_1 = \frac{q_m s_m^2}{9v_m^2}, \quad (20)$$

where

$$\begin{aligned} v_m &= \sum_{\alpha} x_{\alpha} V_{\alpha}, & s_m &= \sum_{\alpha} x_{\alpha} S_{\alpha}, \\ r_m &= \sum_{\alpha} x_{\alpha} r_{\alpha}, & q_m &= \sum_{\alpha} x_{\alpha} q_{\alpha}, \end{aligned} \quad (21)$$

$q_{\alpha} = r_{\alpha}^2$ and the quantities V_{α} , S_{α} , and r_{α} are given in Eqs. (3)-(4), (15). For $\Delta_1 = 1$, the CS correction coincides with the expression used in [24]. In this study, we use the CS correction in the form (20) under the condition that R_2 is the radius of an equivalent HS with the volume which is equal to the volume of the HSC.

Similar to (5), the partial chemical potentials $\beta\mu_{\alpha}^r$ can be written as

$$\beta\mu_{\alpha}^r = \beta\mu_{\alpha}^{\text{CS}} = \beta\mu_{\alpha} + \beta\Delta\mu_{\alpha}^{\text{CS}}, \quad (22)$$

where expressions for $\beta\mu_1$ and $\beta\mu_2$ were derived in [23]. As a result, we have the following expressions for the chemical potential $\beta\mu_1$

$$\begin{aligned} \beta\mu_1^{\text{SPT}} &= \ln \Lambda_1^3 \rho_1 - \ln(1 - \eta) + \frac{1}{2} \frac{\eta}{1 - \eta} \left\{ a_1 + 6 \frac{\rho_1 V_1}{\eta} + \frac{\rho_2 V_1}{\eta} \right. \\ &\times \left[\frac{3}{4} s_1 (1 + 2k_1) + 3k_1 (1 + k_1) \right] \left. \right\} + \frac{1}{3} \frac{\eta^2}{(1 - \eta)^2} \left\{ b_1 + 3 \frac{\rho_1 V_1}{\eta^2} \right. \\ &\times \left[3\eta_1 + \frac{1}{k_1} \frac{6\gamma_2}{3\gamma_2 - 1} \eta_2 \right] + \frac{\rho_2 V_1}{\eta^2} \left[9k_1 \left(\frac{1}{2} s_1 + k_1 \right) \eta_1 \right. \\ &+ \left. \left. \left(\frac{3}{4} \frac{6\gamma_2}{3\gamma_2 - 1} s_1 + 3k_1 \left[3 + \frac{3(\gamma_2 - 1)^2 \delta\tau(f)}{3\gamma_2 - 1} \right] \right) \eta_2 \right] \right\} \\ &+ \beta P V_1, \end{aligned} \quad (23)$$

and for the chemical potential $\beta\mu_2$

$$\begin{aligned}
\beta\mu_2^{\text{SPT}} &= \ln \Lambda_2^3 \rho_2 + \sigma(f) - \ln(1 - \eta) \\
&+ \frac{1}{2} \frac{\eta}{1 - \eta} \left\{ a_2 + \frac{\rho_1 V_2}{\eta} \left[\frac{1}{k_1} \frac{6\gamma_2}{3\gamma_2 - 1} + \frac{1}{2} \frac{1}{k_1^2} \frac{6(\gamma_2 + 1)}{3\gamma_2 - 1} \right] \right. \\
&+ \left. \frac{\rho_2 V_2}{\eta} \left[6 + \frac{6(\gamma_2 - 1)^2 \tau(f)}{3\gamma_2 - 1} \right] \right\} \\
&+ \frac{1}{3} \frac{\eta^2}{(1 - \eta)^2} \left\{ b_2 + \frac{\rho_1 V_2}{\eta^2} \frac{1}{k_1} \frac{6\gamma_2}{3\gamma_2 - 1} \left[3\eta_1 + \frac{1}{k_1} \frac{6\gamma_2}{3\gamma_2 - 1} \eta_2 \right] \right. \\
&+ \left. \frac{\rho_2 V_2}{\eta^2} \left[\left(\frac{3}{4} \frac{6\gamma_2}{3\gamma_2 - 1} s_1 + 3k_1 \left[3 + \frac{3(\gamma_2 - 1)^2 \delta\tau(f)}{3\gamma_2 - 1} \right] \right) \eta_1 \right. \right. \\
&+ \left. \left. \frac{6\gamma_2}{3\gamma_2 - 1} \left(\frac{6(2\gamma_2 - 1)}{3\gamma_2 - 1} + \frac{6(\gamma_2 - 1)^2 \delta\tau(f)}{3\gamma_2 - 1} \right) \eta_2 \right] \right\} + \beta P V_2, \quad (24)
\end{aligned}$$

where the entropic term $\sigma(f)$ is defined as

$$\sigma(f) = \int f(\Omega) \ln f(\Omega) d\Omega \quad (25)$$

and the singlet orientation distribution function $f(\Omega)$ can be obtained from Eqs. (18)-(19).

Based on (7) and (20), we find the expression for $\beta\Delta\mu_\alpha^{\text{CS}}$

$$\begin{aligned}
\beta\Delta\mu_\alpha^{\text{CS}} &= -\frac{V_\alpha}{v_m} \frac{\eta^3}{(1 - \eta)^3} \Delta_1 + \frac{s_m}{9v_m^3} [(q_\alpha s_m + 2S_\alpha q_m)v_m - 2V_\alpha q_m S_m] \\
&\times \left[\ln(1 - \eta) + \frac{\eta}{1 - \eta} - \frac{1}{2} \frac{\eta^2}{(1 - \eta)^2} \right]. \quad (26)
\end{aligned}$$

Putting in the above equations $L_2 = 0$, we obtain the partial chemical potential and pressure for a HS binary mixture.

2.3. Ionic subsystem

The contribution to free energy from the ionic subsystem will be calculated within the framework of the associative mean-spherical approximation (AMSA). In this case, $\Delta f^{\text{ion}} = \Delta F^{\text{ion}}/V$ can be written as [11, 32, 33]

$$\beta\Delta f^{\text{ion}} = \beta f^{\text{mal}} + \beta f^{\text{el}}, \quad (27)$$

where

$$\beta f^{\text{mal}} = \frac{\beta F^{\text{mal}}}{V} = \rho_1 \ln \alpha + \frac{\rho_1}{2} (1 - \alpha) \quad (28)$$

is the contribution from the mass action law (MAL) and

$$\beta f^{\text{el}} = -\frac{\beta e^2}{\varepsilon} \rho_1 \frac{\Gamma^B}{1 + \Gamma^B \sigma_1} + \frac{(\Gamma^B)^3}{3\pi} \quad (29)$$

is the contribution from the electrostatic ion interaction. The degree of dissociation α satisfies the MAL

$$1 - \alpha = \frac{\rho_1}{2} \alpha^2 K, \quad (30)$$

where $K = K^\gamma K^0$ is the association constant with K^0 being the thermodynamic association constant. There is a certain kind of arbitrariness in how we define the ion pair and hence the thermodynamic association constant. Here, K^0 is chosen in the form proposed in [13]. The corresponding association constant K^0 gives the best estimations for the vapour-liquid critical parameters obtained within the framework of the ionic association approach for the bulk RPM [32]. In the AMSA, K^γ is given by [14, 15]

$$K^\gamma = g_{11}(\sigma_1) \exp \left[-b \frac{\Gamma^B \sigma_1 (2 + \Gamma^B \sigma_1)}{(1 + \Gamma^B \sigma_1)^2} \right], \quad (31)$$

where $b = \lambda_B / \sigma_1 = \beta e^2 / \sigma_1 \varepsilon$ is the dimensionless Bjerrum length, Γ^B is the screening parameter calculated from the equation

$$4 (\Gamma^B)^2 (1 + \Gamma^B \sigma_1)^3 = \kappa_D^2 (\alpha + \Gamma^B \sigma_1), \quad (32)$$

where $\kappa_D^2 = 4\pi q^2 \rho_1 / (\varepsilon k_B T)$ is the inverse squared Debye length. It should be noted that without association ($\alpha = 1$), Γ^B reduces to the screening parameter Γ in the MSA [6, 7, 9, 8]

$$\Gamma \sigma_1 = \frac{1}{2} [\sqrt{1 + 2\kappa_D \sigma_1} - 1]. \quad (33)$$

In (31), $g_{11}(\sigma_1)$ is the contact value of the radial distribution function of ions at presence of the solvent molecules. For the solvent molecules modelled by spherocylinders, $g_{11}(\sigma_1)$ is of the form:

$$\begin{aligned} g_{11}(\sigma_1) &= \frac{1}{1 - \eta} + \frac{3}{2} \frac{1}{(1 - \eta)^2} \left(\eta_1 + \frac{1}{k_1} \frac{2\gamma_2}{3\gamma_2 - 1} \eta_2 \right) \\ &+ \frac{1}{2} \frac{1}{(1 - \eta)^3} \left(\eta_1 + \frac{1}{k_1} \frac{2\gamma_2}{3\gamma_2 - 1} \eta_2 \right)^2, \end{aligned} \quad (34)$$

where $\eta = \eta_1 + \eta_2$ is the total volume fraction of ions and solvent molecules, k_1 and γ_2 are given in (13).

Using Eqs. (28) and (30), one obtains the following expressions for P^{mal} and μ_1^{mal} :

$$\beta P^{\text{mal}} = -\frac{\rho_1}{2}(1 - \alpha) \left(1 + \rho_1 \frac{\partial \ln K^\gamma}{\partial \rho_1} \right), \quad (35)$$

$$\beta \mu_1^{\text{mal}} = \ln \alpha - \frac{\rho_1}{2}(1 - \alpha) \frac{\partial \ln K^\gamma}{\partial \rho_1}. \quad (36)$$

For the electrostatic contribution (29), we use the simple interpolation scheme known as the SIS approximation [34]. Within the framework of this approach, the effects of ionic screening are described accurately, but the effects of ionic association are neglected. As a result, one obtains

$$\beta P^{\text{el}} = -\frac{\Gamma^3}{3\pi}, \quad \beta \mu_1^{\text{el}} = -\frac{1}{T^*} \frac{\Gamma \sigma_1}{(1 + \Gamma \sigma_1)}, \quad (37)$$

where Γ is given in (33) and $T^* = b^{-1}$.

Taking into account Eqs. (5)-(25), (35)-(36), and (37), we present pressure and the partial chemical potentials of our system as follows:

$$\beta P^{\text{AMSA}} = \beta P^{\text{CS}} + \beta P^{\text{mal}} + \beta P^{\text{el}}, \quad (38)$$

$$\beta \mu_1^{\text{AMSA}} = \beta \mu_1^{\text{CS}} + \beta \mu_1^{\text{mal}} + \beta \mu_1^{\text{el}}, \quad (39)$$

$$\beta \mu_s^{\text{AMSA}} = \beta \mu_s^{\text{CS}}. \quad (40)$$

These equations are used below for the calculation of phase diagrams. In our calculations, we supplement the AMSA with the SIS [34] substituting Γ (see (33)) for Γ^B in Eqs. (37). This approximation is equivalent to the Wertheim first-order thermodynamic perturbation theory [35]. The approach gives a reasonable estimate for the location of the critical point of the RPM fluid.

Neglecting in (38)-(39) the addends connected with associations one arrives at the pressure and the chemical potentials in the MSA.

3. Results and Discussion

We consider two models – a binary mixture of RPM and HSC particles (RPM-HSC) and a binary mixture of the RPM and HS particles (RPM-HS). In the latter model, the volume of a solvent particle (neutral HS) is taken

of the same value as the one of a hard spherocylinders (neutral HSC) in the former model. According to the condition of equality of the HSC and HS volumes ($V_2^{HS} = V_2^{HSC}$) and using (3)-(4) the following relationship between the diameters of HS and HSC solvent particles ($\sigma_2 = 2R_2$) can be derived in the following form:

$$\sigma_2^{\text{HS}} = \sigma_2^{\text{HSC}}[(3\gamma_2 - 1)/2]^{1/3}, \quad (41)$$

where γ_2 is given in (13). In this study, we consider spherocylinders with $L_2 = 5\sigma_1$ (where $\sigma_1 = 2R_1$), then the diameter of an equivalent HS is equal to $2.0408\sigma_1$.

In this section we present results for the phase diagrams obtained from both the MSA and the AMSA. Coexistence curves are calculated at subcritical temperatures using the conditions of two-phase equilibrium

$$\mu_i(\rho^\alpha, x_1^\alpha, T) = \mu_i(\rho^\beta, x_1^\beta, T), \quad (42)$$

$$\mu_s(\rho^\alpha, x_1^\alpha, T) = \mu_s(\rho^\beta, x_1^\beta, T), \quad (43)$$

$$P(\rho^\alpha, x_1^\alpha, T) = P(\rho^\beta, x_1^\beta, T), \quad (44)$$

where $\rho^{\alpha(\beta)}$ is the total number density ($\rho = \rho_1 + \rho_2$) in phase $\alpha(\beta)$ and $x_1^{\alpha(\beta)}$ is the concentration in phase $\alpha(\beta)$ of ions, $x_1 = \rho_1/\rho$. The phase diagrams are built by solving numerically a set of equations Eqs. (42)-(44) with respect to the densities ρ^α and ρ^β and one of the concentrations x_1^α when the second concentration x_1^β is given. Therefore, a series of the densities and concentrations in phases α and β are obtained at temperatures of wide range. To solve the set of equations Eqs. (42)-(44), the Newton-Raphson iterative procedure has been used with an accuracy 10^{-9} . In the following, length is measured in σ_1 units and we introduce dimensionless units for the temperature, pressure, and total number density

$$T^* = k_B T \varepsilon \sigma_1 / e^2, \quad P^* = P \varepsilon \sigma_1^4 / e^2, \quad \rho^* = \rho \sigma_1^3. \quad (45)$$

First, we calculate the phase diagrams in the MSA. In this case, we neglect in Eqs. (38)-(39) the contributions connected with the MAL. In Figs. 1 (a)-(b), we show the coexistence curves which are calculated at the selected pressures using Eqs. (42)-(44) and presented in the T^* - ρ^* and T^* - x_1 planes ($x_1 = \rho_1/\rho$ is the concentration of ions). The considered pressures are higher than the critical pressure of the RPM in the MSA ($P^* = 9.64 \times 10^{-5}$). It is worth noting that the MSA predictions for the critical temperature

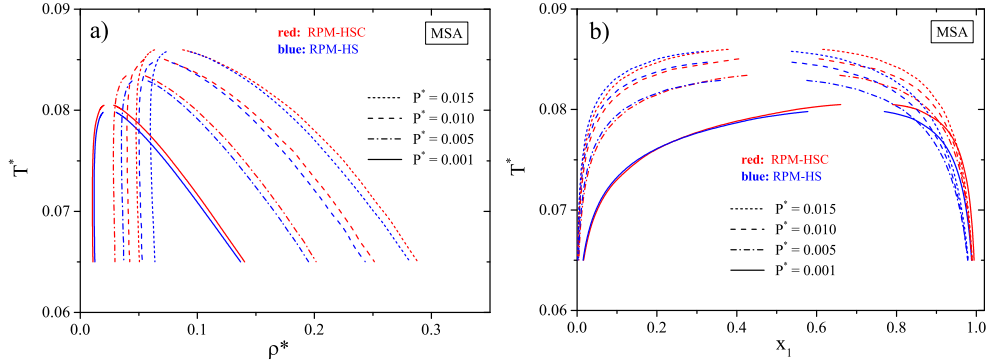


Figure 1: Coexistence curves of the RPM/HSC and RPM/HS mixtures in T^* - ρ^* (a) and T^* - x_1 (b) planes at constant reduced pressures in the MSA approximation. T^* , P^* , and ρ^* are defined in Eq. (45), and $x_1 = \rho_1/\rho$.

and the critical density of the RPM are as follows [36]: $T_c^* = 0.07858$ and $\rho_c^* = 0.01449$. As one can see from Fig. 1 (a), an increase of pressure shifts the coexistence region towards higher total number densities and towards higher reduced temperatures. Simultaneously, the width of the coexistence region becomes larger. This behaviour is observed for the both models, RPM-HSC and RPM-HS. However, the coexistence envelopes in the case of the RPM-HSC mixture (red curves) are broader than those in the case of RPM-HS mixture (blue curves). Broadening of the coexistence region with an increase of pressure is also observed for the both models in the T^* - x_1 plane (Fig. 1 (b)). As in Fig. 1 (a), the coexistence envelopes of the RPM-HSC mixture (red curves) are wider than those of the RPM-HS mixture (see Fig. 1 (b)). At the same time, this difference is more essential for the ion rich branches than for the ion poor branches. One can also notice that the critical concentration of ions decreases with increasing pressure.

Now, let us consider the phase diagrams obtained from the AMSA theory. In this case, the partial chemical potentials and pressure are given by Eqs. (35)-(40) supplemented by the solution of Eq. (32). The association constant is chosen to be $K^0 = 12K_{Eb}^0$ (K_{Eb}^0 is the association constant introduced by Ebeling [37, 33]). As in the MSA, the selected values of pressure are higher than the critical pressure of the RPM. The reduced critical parameters of the RPM calculated in the AMSA are as follows [32]: $T_c^* = 0.0492$, $P_c^* = 7.44 \times 10^{-4}$, and $\rho_c^* = 0.059$. It should be noted that the critical pres-

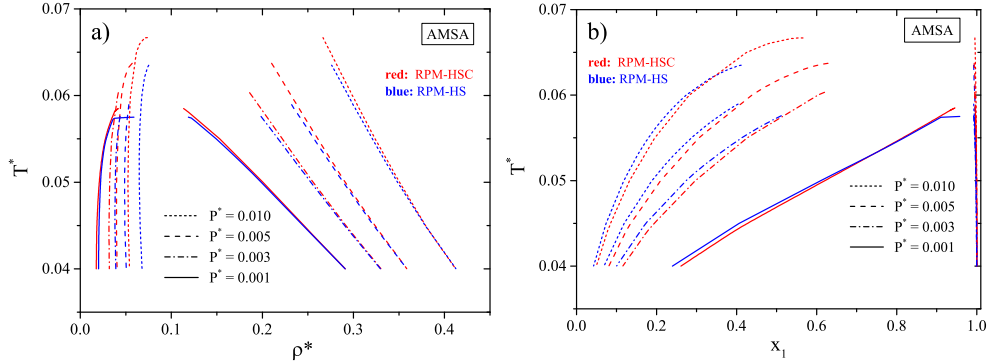


Figure 2: Coexistence curves of the RPM/HSC and RPM/HS mixtures in T^* - ρ^* (a) and T^* - x_1 (b) planes at constant reduced pressures in the AMSA approximation. T^* , P^* , and ρ^* are defined in Eq. (45), and $x_1 = \rho_1/\rho$.

sure of the RPM obtained from the AMSA theory is by an order higher than the corresponding pressure found from the MSA. Accordingly, for the RPM, the AMSA critical density is by four times higher than the critical density obtained from the MSA.

In Figs. 2 (a)-(b), we present the coexistence curves calculated using the AMSA theory. In general, the trends of the (T^*, ρ^*) phase diagrams (Fig. 2 (a)) with an increase of pressure are similar to the corresponding trends found in the MSA, although some deviations are observed. In the AMSA, the difference between the high-density branches obtained for the RPM-HSC and RPM-HS mixtures slightly increases with an increase of temperature (Fig. 2 (a)) while an opposite trend is found in the MSA (see Fig. 1 (a)). Different trends have been also noticed in the critical region. Nevertheless, in the most cases the critical temperature in the RPM-HSC system is higher than in the RPM-HS system, and one can see that at the higher pressures it becomes almost identical for the both models within the MSA, while in the AMSA the difference between critical temperatures of the RPM-HSC and RPM-HS remains essential at all considered pressures. The differences between the results obtained in the MSA and AMSA appear due to the MAL term in the AMSA theory, which takes into account the associative interaction caused by strong attraction between positively and negatively charged ions of RPM. Moreover, the MAL contribution depends on the contact value between ionic particles (34), and it strongly depends on

the densities and concentrations in the system. At same time, the strength of association is also defined by the temperature.

Regarding the (T^*, x_1^*) diagrams obtained in the AMSA (Fig. 2 (b)), they substantially differ from those shown in Fig. 1 (b). Contrary to the MSA results, the phase diagrams obtained for the both models from the AMSA show that the high-density phase mostly consists of ions at all the considered values of pressure. Therefore, the effects of association between ions being taken into account can lead to the phase diagrams which differ qualitatively from the phase diagrams calculated in the MSA.

It should be noted that we have not observed any isotropic-nematic phase transition in the RPM-HSC system, i.e. in all our calculations HSC particles have been in the isotropic state. This is because at the given parameters, the density and concentration of HSC particles do not reach appropriate values at which the nematic phase can form. For instance, it is known [24] (case $L_2 = 5.0\sigma_2$) that for the pure HSC system ($x_1 = 0$), a stable nematic phase appears at the HSC density around 0.094. One can see that in the ion poor regions, where x_1 is rather small, the density of HSC particles is far lower than 0.094. Furthermore, it was found from the SPT for the binary mixture of uncharged HS and HSC particles [24] that the nematic phase cannot be formed at all if the concentration of HS particles is higher than 0.4. As it is seen from our diagrams, the concentration of ions x_1 is always higher than 0.4, where the density ρ^* is larger than 0.094. However, we cannot exclude a possibility of the isotropic-nematic phase transition in RPM-HSC systems with an increasing pressure, where the particles should be packed denser, or for the longer HSC particles, where the nematic phase can exist at lower densities. Moreover, in this case one can obtain more than two coexisting phases simultaneously, i.e., apart from the lower density isotropic phase one can observe a higher density isotropic phase and a higher density nematic phase. This point needs a more comprehensive study.

4. Conclusion

We have studied the fluid-fluid phase behaviour of the explicit solvent model represented as a binary mixture of oppositely charged HS of equal diameters (RPM) and neutral hard spherocylinders (HSC). To describe this model, we have proposed the approach combining the SPT theory and the AMSA approximation, and on this basis we have derived the expressions for the partial chemical potential and pressure. More specifically, the thermody-

dynamic properties of the reference system represented as a binary mixture of neutral HS and neutral HSC has been obtained using the SPT approach. For an ionic subsystem we have used the SIS-AMSA theory, which corresponds to the Wertheim first-order thermodynamic perturbation theory. For comparison, the ionic subsystem has been also treated within the MSA theory.

We have considered two models: the RPM-HSC mixture and an “equivalent” RPM-HS mixture. In the former case, we have restricted our attention to the HSC with an aspect ratio $L_2/\sigma_2 = 5$ and RPM particles of diameter $\sigma_1 = \sigma_2$. In the latter model, the solvent is represented as HS particles with the volume equal to the volume of the HSC particles of the former case. It is known that for totally uncharged mixtures of HSC and HS, at low densities, HSC component exists in isotropic state, i.e., no orientation order is expected. At sufficiently high densities, a HSC component can form the nematic phase, and due to a subtle balance between entropic contributions from different components, the demixing phenomena can take place, where the HSC and HS start to redistribute between nematic and isotropic phases [24, 38, 39]. We have not found the nematic phase in the RPM-HSC model at pressures considered in the present study. However, our preliminary results suggest a possibility of isotropic-nematic phase transitions at higher pressures or/and longer HSC particles. This requires a more thorough investigation, which will be done in future studies.

We have calculated the fluid-fluid coexistence curves of the RPM-HSC and RPM-HS mixtures using the equations of phase equilibrium. The analysis of the results have demonstrated that both models show a similar fluid-fluid phase behaviour although quantitative difference exists. It is seen from the MSA phase diagrams that the critical temperature increases with an increase of pressure and this dependence is more noticeable than in the case of an equisized RPM-HS mixture (see [3]). Although we have not managed to get the critical points in the AMSA, it is clearly seen that the coexistence envelopes of the RPM-HSC and RPM-HS mixtures obtained from the both theories shift towards higher total number densities and towards higher reduced temperatures when the pressure increases. Simultaneously, the coexistence envelopes become broader. At the same time, the AMSA and MSA phase diagrams of the both models presented in the temperature-concentration plane considerably differ. The AMSA phase diagrams show that the high-density phase mostly consists of the ions for all pressures considered in this study. This result also differs from the results recently obtained for the RPM-HS mixture with $\sigma_1 = \sigma_2$ [3] where similar situation was observed only for low

pressures.

To the best of our knowledge, we have made the first attempt to theoretically describe the fluid-fluid equilibrium in an explicit solvent model in which the solvent molecules are of non-spherical shape. We have shown the effect of asphericity of solvent molecules on the phase behavior in such systems. It was shown that at the given parameters, the considered RPM-HSC model was in isotropic state. However, the effect of asphericity of solvent molecules can be more essential if the fluid-fluid phase transition is accompanied by the isotropic-nematic phase transitions. Hence, we suggest to consider the higher pressures and longer spherocylinder particles. It is also important to take into account attractive interactions between solvent particles, or/and an attraction between solvent molecules and ions.

Acknowledgement

This work was partly supported by the European Union's Horizon 2020 research and innovation programme under the Marie Skłodowska-Curie grant agreement No 734276.

References

- [1] P.U. Kenkare, C.K. Hall, C. Caccamo, *J. Chem. Phys.*, **103** (1995) 8098-8110.
- [2] Y. Zhou, G. Stell, *J. Chem. Phys.*, **102** (1995) 5796-5802.
- [3] O.V. Patsahan, T.M. Patsahan, *J. Mol. Liq.*, **275** (2019) 443-451.
- [4] D. Chandler D., H.C. Andersen, *J. Chem. Phys.* **54** (1971) 26-33.
- [5] J. D. Weeks, D. Chandler, H.C. Andersen, *J. Chem. Phys.* **54** (1971) 5237-5247.
- [6] E. Waisman, J.L. Lebowitz, *J. Chem. Phys.*, **56** (1972) 3086-3093.
- [7] E. Waisman, J.L. Lebowitz, *J. Chem. Phys.*, **56** (1972) 3093-3099.
- [8] L. Blum, *Mol. Phys.*, **30** (1975) 1529-1535.
- [9] L. Blum, *J. Chem. Phys.*, **61** (1974) 2129-2133.

- [10] M.F. Holovko, Yu.V. Kalyuzhnyi, *Mol. Phys.* **73** (1991) 1145-1157.
- [11] M.F. Holovko, in: D. Henderson, M. Holovko, A. Trokhymchuk (eds.), *Ionic Soft matter: Modern trends in theory and applications*, Springer, Dordrecht, Netherlands, 2005, 206, pp. 45-81.
- [12] T. Kristóf, D. Boda, I. Szalai, D. Henderson, *J. Chem. Phys.*, **113** (2000) 7488-7491.
- [13] K. Olaussen, G. Stell, *J. Stat. Phys.*, **62** (1991) 221-237.
- [14] L. Blum, O. Bernard, *J. Stat. Phys.*, **79** (1995) 569-583.
- [15] O. Bernard, L. Blum, *J. Chem. Phys.*, **104** (1996) 4746-4754.
- [16] H. Reis, H. Frisch and J. L. Lebowitz, *J. Chem. Phys.*, **31** (1959) 369-380.
- [17] H. Reis, H. Frisch, E. Helfand and J. L. Lebowitz, *J. Chem. Phys.*, **32** (1960) 119-124.
- [18] R. M. Gibbons, *Mol. Phys.*, **17** (1969) 81-86.
- [19] M. A. Cotter and D. E. Martire, *J. Chem. Phys.*, **52** (1970) 1902-1908.
- [20] M. A. Cotter and D. E. Martire, *J. Chem. Phys.*, **53** (1970) 4500-4511.
- [21] M. A. Cotter, *Phys. Rev. A*, **10** (1974) 625-636.
- [22] M. Holovko, V. Shmotolokha, T. Patsahan, *J. Mol. Liq.*, **189** (2014) 30-38.
- [23] M.F. Holovko, M.V. Hvozd, *Condens. Matter Phys.*, **20** (2017) 43501: 1-11.
- [24] M. Hvozd, T. Patsahan, M. Holovko, *J. Phys. Chem. B*, **122** (2018) 5534-5546.
- [25] J. D. Parsons, *Phys. Rev. A*, **19** (1979) 1225-1230.
- [26] S. D. Lee, *J. Chem. Phys.*, **87** (1987) 4972-4974.
- [27] N.F. Carnahan, K.E. Starling, *J. Chem. Phys.*, **51** (1969) 635-636.

- [28] G. A. Mansoori, N. F. Carnahan, K. E. Starling, T. Leland, J. Chem. Phys., **54** (1971) 1523-1525.
- [29] T. Boublík, Mol. Phys. **27** (1974) 1415-1427.
- [30] T. Boublík, J. Chem. Phys. **63** (1975) 4084.
- [31] M. Holovko, V. Shmotolokha, T. Patsahan, in "Physics of Liquid Matter: Modern Problems" ed. by Bulavin L. and Lebovka N. Springer Proceedings in Physics, vol. 171, Heidelberg, 2015.
- [32] J. Jiang, L. Blum, O. Bernard, J.M. Prausnitz, S.I. Sandler, J. Chem. Phys., **116** (2002) 7977-7982.
- [33] M. Holovko, T. Patsahan, O. Patsahan, J. Mol. Liq. **228** (2017) 215-223.
- [34] G. Stell, Y.Q. Zhou, J. Chem. Phys., **91** (1989) 3618-3623.
- [35] M.S. Wertheim, J. Stat. Phys., **35** (1984) 35-47.
- [36] J.-M. Caillol, Mol. Phys. **103** (2005) 1271-1283.
- [37] W. Ebeling, Z. Phys. Chem. (Leipzig), **238** (1968) 400-402.
- [38] A. Cuetos, B. Martínez-Haya, S. Lago, L.F. Rull, Phys. Rev. E, **75** (2007) 061701-12.
- [39] S. Lago, A. Cuetos, B. Martínez-Haya, L.F. Rull, J. Mol. Recognit., **17** (2004) 417-425.